Investigation on Switching Operation in Resistive RAM Using In-Situ TEM

Masashi Arita and Yasuo Takahashi

Abstract Our recent works on resistive RAMs (ReRAMs) are reviewed, where in-situ transmission electron microscopy (TEM) realizing simultaneous electric measurements and TEM observations was applied to investigate resistive switching operation of some conductive bridging RAMs (CBRAMs). In multiple switching cycles, the Cu conductive filament was experimentally confirmed to appear in the *Set* process giving the low resistance state (LRS, on-state) and to disappear in the *Reset* process giving the high resistance state (HRS, off-state). No drastic change in the geometry of the conductive filament was seen when the switching current was small. With increasing the current, the filament became thick, but its position was unstable, and too much Cu moved into the switching layer in a wide area. This may induce the device degradation and failure.

1 Introduction

Large resistance change with voltage application was widely known in Perovskite type complex oxides, binary oxides such as NiO, TiO_2, HfO_2 and Ta_2O_5, and solid electrolyte (e.g. Ge-S) with Cu or Ag. In recent years, many works have been reported to apply this phenomenon on non-volatile resistive RAMs (ReRAMs) and on neuromorphic devices [1–4]. To guarantee the operation of these devices, clarification of the switching mechanism is strongly required. Based on the electrochemical discussion of their electric properties, it is a common knowledge that the resistance switching in binary oxides and solid electrolytes is caused by formation and rupture of the conductive filament [1, 2]. However, details of its operation mechanism are still ambiguous and difficult to be clarified only using electric properties. Dynamical observations in real space using in-situ transmission electron microscopy (TEM) are a method to overcome this difficulty, where the

M. Arita (✉) · Y. Takahashi
Graduate School of Information Science and Technology, Hokkaido University,
Kita-14, Nishi-9, Kita-ku, Sapporo 060-0814, Japan
e-mail: arita@nano.ist.hokudai.ac.jp

© Springer International Publishing AG 2017

A.Y. Oral and Z.B. Bahsi Oral (eds.), *3rd International Multidisciplinary Microscopy and Microanalysis Congress (InterM)*, Springer Proceedings in Physics 186,
DOI 10.1007/978-3-319-46601-9_24

electric measurements and TEM observations can be performed synchronously [5–10]. Several types of in-situ TEM holders became commercially available in recent years, and the number of reports in this category has increased. However, works on realistic switching operations such as the current-voltage (*I-V*) switching cycle, the switching repetition and the pulse endurance are rare [11, 12].

In this report, our recent works on ReRAMs using the in-situ TEM are reviewed, which are categorized as the conductive bridging RAM (CBRAM) such as GeS-Cu [13, 14], Cu/MoO_x [11, 15, 16] and Cu/WO_x [17, 18]. In all of these CBRAM systems, the Cu conductive filament was experimentally confirmed to appear in the *Set* process giving the low resistance state (LRS, on-state) and to disappear in the *Reset* process giving the high resistance state (HRS, off-state). No drastic change in the geometry of the conductive filament was seen at the *Set*/*Reset* switching moment, and the filament growth/erasure was seen during continuation of the current flow.

2 Experimental Procedure

Three types of ReRAMs were used for investigation, which were composite GeS-$Cu_{(8–60\ nm)}$ deposited on a wedge-shaped PtIr, $Pt_{(100\ nm)}$/$Cu_{(30\ nm)}$/$MoO_{x(50nm)}$ or $Pt_{(100nm)}$/$Cu_{(30nm)}$/$WO_{x(20nm)}$ trilayer films on a TiN/Si wafer chip. For all samples, the film deposition was done using conventional RF sputtering (Ar) or reactive sputtering (Ar-20 %O_2) of metal targets at room temperature (RT). In the latter two samples, the Cu and the TiN layers worked as the top electrode (TE) and the bottom electrode (BE), respectively. The GeS-Cu sample was used for in-situ TEM without any further processing, because the tip of the PtIr wedge was thin enough for TEM observations. On the other hand, the ReRAM samples of MoO_x and WO_x were processed using the ion-shadow method [19] which is a kind of the ion-milling method.

In-situ TEM experiments were carried out using the system shown in Fig. 1 composed of a hand-made piezo-driven TEM holder and a JEM-2010 microscope (C_s = 0.5 mm). A movable Pt-Ir probe was contacted to one of the ReRAM devices formed on the TEM sample, and the *I-V* switching cycles were measured using a commercially available source-measure-unit (SMU, Yokogawa GS610). To prevent eternal device destruction caused by the strong overshoot current in the *Set* process, current limitation (compliance current; I_{comp}) was introduced using this SMU. In the GeS-Cu sample, the wedge-shaped PtIr substrate was biased while the probe was grounded. On the other hand, in MoO_x and WO_x samples, the TiN/Si substrate was grounded while the probe was biased. Geometrical change of the filament was dynamically recorded using a CCD camera (30 ms/frame).

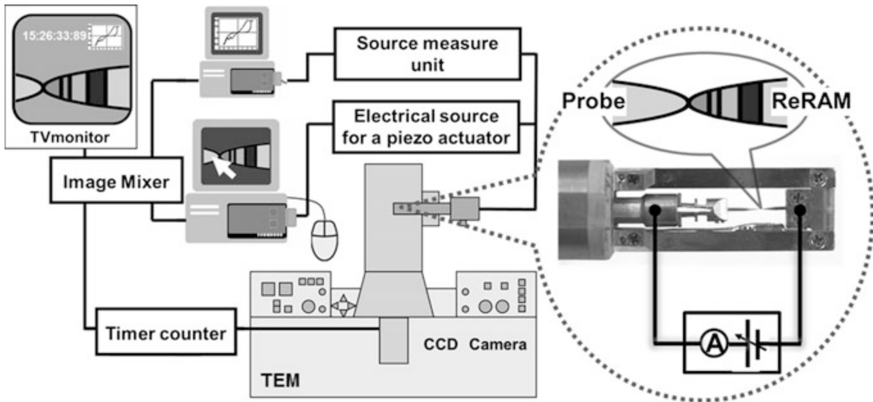

Fig. 1 In-situ TEM system

3 Results and Discussion

3.1 Filament Formation in Cu-GeS

The *I-V* curve measured in TEM is shown in Fig. 2, where the horizontal axis corresponds to the potential of the substrate relative to the probe [13, 14]. The voltage was varied in a sequence of 0 V, +7 V, −2 V and 0 V, and a clear hysteresis curve was obtained. Though the retention time (memory holding time) of the LRS was not long enough for the practical memory application, formation and erasure of the conductive filament was clearly confirmed.

The TEM images extracted from the video are shown in Fig. 3. There are a Cu-GeS amorphous film containing Ge nanocrystals on the Pt-Ir substrate (Fig. 3a). In the first quadrant of the *I-V* graph, where the substrate was positively biased

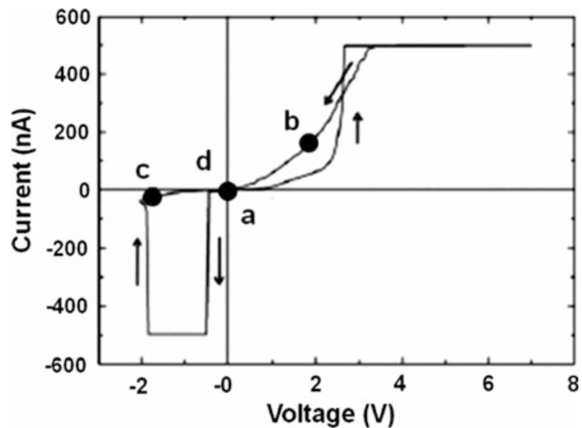

Fig. 2 *I-V* curve of Cu-GeS

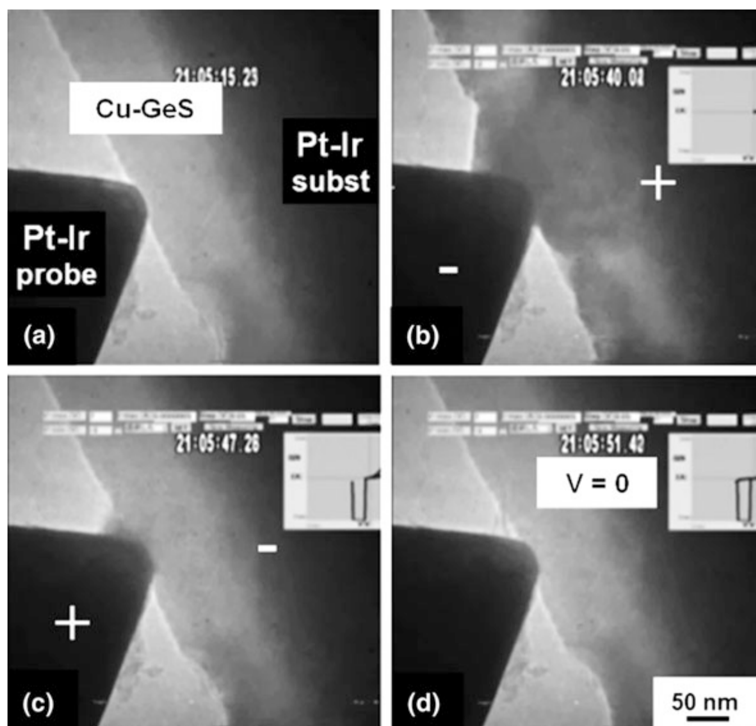

Fig. 3 Microstructure corresponding to Fig. 2. Video **a** in the initial state, **b** and **c** with positive or negative voltage, and **d** after the *I-V* cycle

relative to the probe, the current increased gradually. There was drastic increase at the voltage of +2.6 V, and its resistance was converted to the LRS (*Set* operation). Correspondingly to this change, a filamentary dark contrast appeared (Fig. 3b). In the selected area diffraction (SAD) pattern during the *Set* process, Debye rings of Cu appeared. In addition, the energy dispersive X-ray spectroscopy (EDX) measurements were done during the *Set* process with positive bias voltage to the substrate (but on another filament than that in Fig. 3). In Fig. 4, the EDX spectra before (Fig. 4a) and during (Fig. 4b) the *Set* operation are compared. It was clearly identified that the deposit contained much Cu. Considering these two results, the deposit appeared in the *Set* process was concluded to be made of Cu nanocrystals. Afterwards, a negative voltage sweep was done, and the deposit gradually disappeared and completely erased at about −2.8 V (Fig. 3c, d). The resistance showed a sudden increase at this moment. This is the *Reset* process which converts the LRS to the HRS. The deposit observed here worked as a conductive filament for the CBRAM switching.

Repeating switching cycles, the *Set* voltage (V_{set}) gradually decreased. This indicates that the Cu-GeS layer in the HRS after the *Reset* operation changed from the initial state as confirmed in Fig. 5. First, a filament was formed (Fig. 5a) and

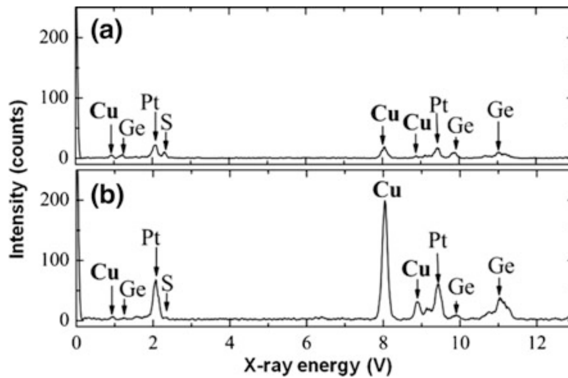

Fig. 4 EDX spectra **a** without and **b** with positive voltage application. The deposit contained much more Cu than other regions

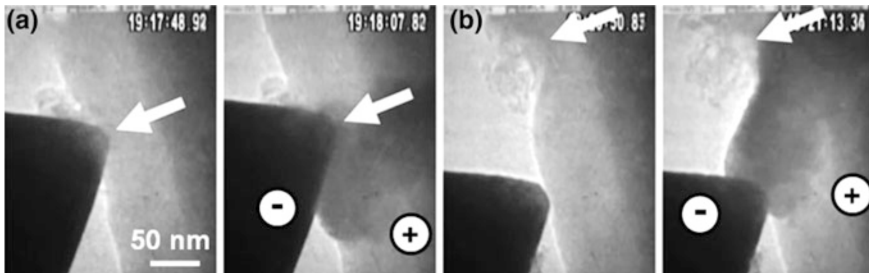

Fig. 5 Filament growth in sequential switching cycles (**a** and **b**), where *arrows* indicate corresponding position. In each figure, the *left panel* is before the switching cycle, and the *right panel* is with positive voltage. The filament appeared almost in same place

erased. Afterwards, the Pt-Ir probe was shifted by 100 nm (Fig. 5b left panel), and a positive voltage was applied to generate a filament again (Fig. 5b right panel). The filament appeared from the probe toward the position of the first filament. It did not reach the nearest position on the substrate. The region in which the filament was formed once must be a priority position for the formation and the growth of a filament. It is expected that there are some residuals such as Cu nanocrystals even after filament erasure, which can behave as filament nuclei. This is thought to make the filament formation easy and to induce reduction of V_{Set}.

The results mentioned above suggest that the Cu filament is formed/erased by application of positive/negative voltage, and the CBRAM operation is achieved. Checking the TEM video, the filament grew from the probe (negative voltage side) with positive voltage, and it was ruptured and erased from the substrate (negative voltage side) with negative voltage. This dynamics fits to the electrochemical model (ECM) reported so far, where the Cu ions drifted along the electric field are reduced to be the metal by receiving electrons on the cathode surface, and the Cu filament is

formed towards the anode [1]. However, the current was small (<1 μA), and the retention property of the LRS was not good enough. The probe used as the BE was mechanically contacted to the solid electrolyte switching layer (Cu-GeS), and this is different from the realistic CBRAM device. To investigate more realistic switching operation, a Cu/MoO_x/TiN trilayer CBRAM will be discussed in the next subsection.

3.2 Set/Reset Switching of Cu/MoO_x/TiN

The sample was Pt/Cu/MoO_x/TiN/Si where Cu and TiN were the TE and BE, respectively [11, 15, 16]. The device size was 350 nm in diameter. The electric properties were measured between the Pt cap layer (biased) and the Si substrate (grounded). An example of the *I-V* curve is shown in Fig. 6a, which was the second switching cycle after the initialization process called as *Forming*. A shaper *Set* than in Cu-GeS is seen in the first quadrant. The corresponding TEM images extracted from a video are presented in Fig. 6b. The resistance state was the HRS between the states A and B, and there was no clear change in the image. Just after the *Set* switching (state C), a small dark region (nucleus of the filament) appeared near the TiN BE. Though the current was almost the compliance value (I_{comp}), there was no dark region binding the TE and BE. The ionic current of the Cu anion is thought to contribute to electric conduction. Afterwards, the filament grew from the TiN BE towards the Cu TE. The bridging of the filament between the TE and the BE was completed within 200 ms.

The *Reset* operation was started at 5 min. after the *Set* process was completed. The LRS was kept after this interval, because I_{comp} was large (400 μA). Two small current jumps between −1 and −2 V in Fig. 6a correspond to the *Reset* switching. The *Reset* curve was uneven as frequently observed in conventional CBRAM devices. This may suggest that *Reset* is more complicated process than *Set*. In the corresponding TEM image (Fig. 6b), there is no clear structure change just after *Reset* switching (state F). This switching is thought to occur very locally, and it was

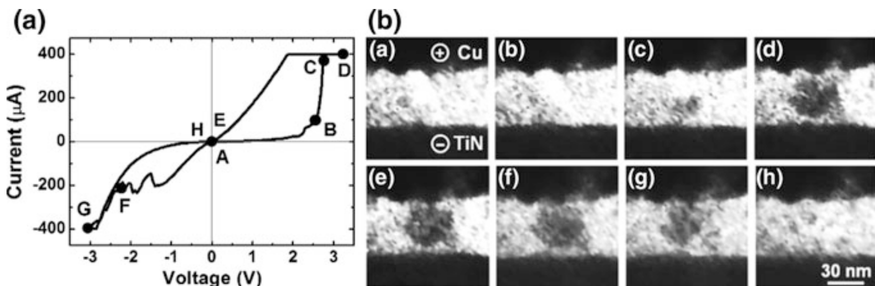

Fig. 6 **a** I-V characteristics of Cu/MoO_x/TiN and **b** TEM images during in-situ observation

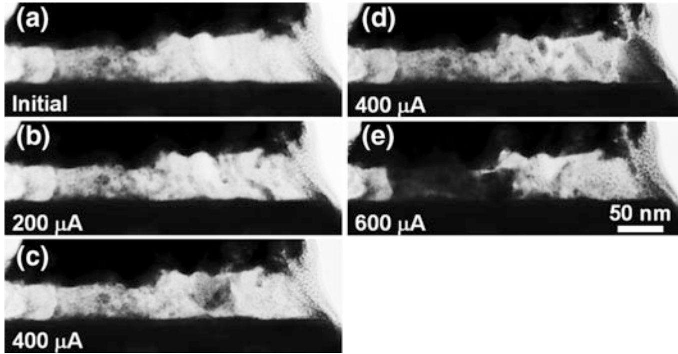

Fig. 7 TEM images of Cu/MoO_x/TiN. **a** Initial state and **b–e** LRS with increasing I_{comp}

not identified in the TEM image. Increasing negative current to about −300 μA (at −2.6 V), the filament was ruptured near the interface between MoO_x and TiN and shrank toward the Cu TE (states G). This process with additional negative current is called the *over-Reset* process in this report. The filament erasure here cannot be explained by the ECM model where the filament shrinks from the Cu TE to the BE. In the present work, the surface of the TiN BE was oxidized. The resistance at this oxidized region is high, and the local temperature must increase by Joule heating. Thus, it is thought that the electrochemical reaction of Cu in this region preferentially occurred, and the Cu filament shrank toward the TE. The current of 100 μA (or more) was used for switching operation in many CBRAM devices reported earlier. While the details are still obscure, it must be sure that the Joule heat influences the *Reset* operation.

In this paragraph, the filament position and size will be discussed. Images after *Set* of five switching cycles are compared in Fig. 7, where I_{comp} was increased stepwise. Here, the filament was almost completely erased by performing *over-Reset*. The initial state was the HRS, and the contrast in Fig. 7a is due to the matters such as the outer shape of the specimen. In the first switch with I_{comp} = 200 μA, a filament having a width of 7 nm was formed (Fig. 7b). By increasing I_{comp}, the filament width increased to 35, 45 and 100 nm in Figs. 7c–e respectively. This increase can be used for the multi-bit memory operation. However, the filament position changed as seen in these figures. This position instability is thought to be caused by almost complete filament erasure during *over-Reset*.

3.3 Device Degradation of Cu/WO_x/TiN

The investigated sample was Pt/Cu/WO_x/TiN/Si [17, 18]. Examples of *I-V* graphs measured during in-situ TEM are shown in Fig. 8a–c where the horizontal axis denotes the potential of the Cu electrode relative to TiN/Si. Figure 8a is the

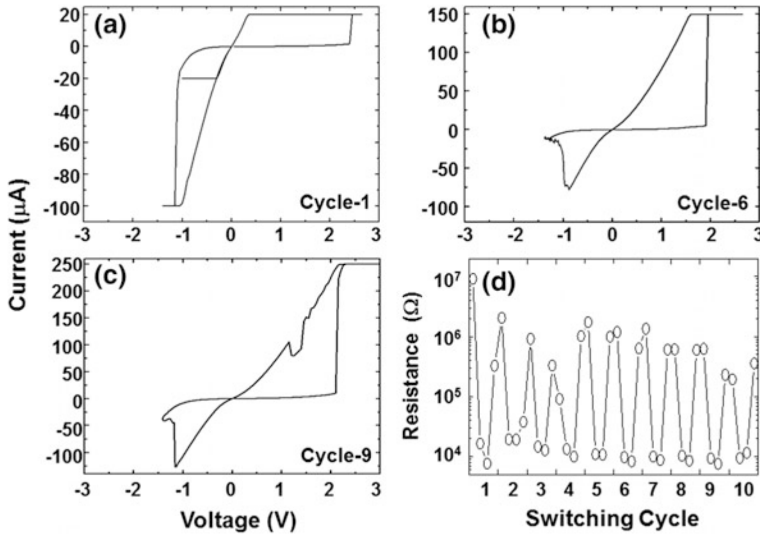

Fig. 8 **a**–**c** *I-V* curves during in-situ TEM of Cu/WO_x/TiN and **d** the cyclic endurance where the resistance was estimated at ±0.3 V

Forming curve. There was a current jump at 2.4 V. This resistance change to the LRS was much quicker than in MoO_x. Correspondingly, a filament was formed between the Cu and TiN electrodes within one video frame (30 ms). The LRS was kept just before the *Reset* operation which was performed at 9.5 min after *Set*, and the retention time was long enough for *in-situ* TEM experiments. By carefully checking the video during the *Reset* operations, clear filament erasure was not identified though sharp switching to the HRS was realized. No strong *over-Reset* was adopted in this switching series as seen in Fig. 8b, c, and thus the filament was not erased (but with switching to the HRS). This result suggests that ReRAM switching occurs in local area of the filament. The resistance change in switching repetition (endurance graph) is shown in Fig. 8d. The resistance ratio of HRS/LRS was kept about 100, and a reasonable CBRAM endurance property is seen. However, as seen in this graph, the resistance in the HRS gradually decreased with the switching cycle. This degradation is known also in realistic ReRAM devices, and it has been reported to induce the endurance failure where the ReRAM switching cannot be achieved [20, 21]. This is believed to be caused by imbalance between *Set* and *Reset*. In Fig. 9, TEM images after *Set*/*Reset* switching cycles are compared. During switching repetition with increasing I_{comp}, Cu moved into the WO_x layer in a wide area, and the effective thickness of the WO_x layer became thin. This is thought to be the origin of the endurance failure.

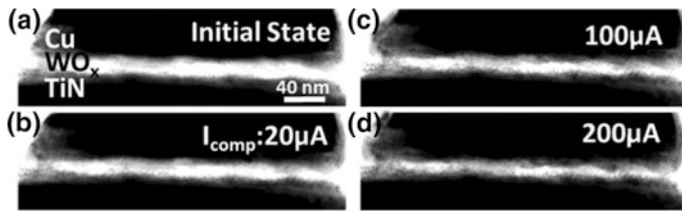

Fig. 9 TEM images of Cu/WO_x/TiN. **a** Initial state and **b–e** LRS after the continuous *Set* operations with increasing compliance current

4 Conclusion

In this work, in-situ TEM was applied on three CBRAMs to investigate the microstructure during the switching operation. It was experimentally confirmed that the Cu filament is formed in *Set*, ruptured in *Reset* and erased in *over-Reset*. The filament becomes thick with increasing the operation current, but its position becomes instable. It was also confirmed that Cu moved into the solid electrolyte and thinned the switching layer. This reduces the resistance of the HRS and finally induces the endurance failure. The retention property must improve by increasing the *Set* current, and large resistance ratio of HRS/LRS is expected by *over-Reset*. However, these treatments induce instability of the filament position and movement of excess Cu in wide area. These can be origins of device failure. Selection of materials and the device structure for easy *Set*/*Reset* balancing must be important for further development of ReRAM devices.

Acknowledgments This work was supported by KAKENHI by JSPS (Nos. 25420279, 26630141, 15H01706) and the Mitsubishi Foundation. Part of this work was collaborated with STARC and Cooperative Research Program of “Network Joint Research Center for Materials and Devices”. Support by the Nanotechnology Platform Program is also acknowledged. We are also grateful to our laboratory members for collaboration.

References

1. Waser, R., Aono, M.: Nanoionics-based resistive switching memories. Nat. Mater **6**, 833–840 (2007). doi:10.1038/nmat2023
2. Akinaga, H., Shima, H.: Resistive random access memory (ReRAM) based on metal oxides. Proc. IEEE **98**, 2237–2251 (2010). doi:10.1109/JPROC.2010.2070830
3. Prezioso, M., Merrikh-Bayer, F., Hoskins, B.D., Adam, G.C., Likharev, K.K., Strukov, D.B.: Training and operation of an integrated neuromorphic network based on metal-oxide memristors. Nature **521**, 61–64 (2015). doi:10.1038/nature14441
4. DeSalvo, B., Vianello, E., Garbin, D., Bichler, O., Perniola, L.: From memory in our brain to emerging resistive memories in neuromorphic systems. In: Proceedings of 7th International Memory Workshop (IMW), pp. 9–12. IEEE, Piscataway (2015). doi:10.1109/IMW.2015.7150286

5. Fujii, T., Kaji, H., Kondo, H., Hamada, K., Arita, M., Takahashi, Y.: I-V hysteresis of $Pr_{0.7}Ca_{0.3}MnO_3$ during TEM observation. IOP Conf. Ser. Mater. Sci. Eng. **8**, 012033 (2010). doi:10.1088/1757-899X/8/1/012033
6. Kwon, D.-H., et al.: Atomic structure of conducting nanofilaments in TiO_2 resistive switching memory. Nat. Nanotechnol. **5**, 148–153 (2010). doi:10.1038/NNANO.2009.456
7. Fujii, T., et al.: I-V measurement of NiO nanoregion during observation by transmission-electron microscopy. J. Appl. Phys. **109**, 053702 (2011). doi:10.1063/1.3553868
8. Choi, S.-J., et al.: In situ observation of voltage-induced multilevel resistive switching in solid electrolyte memory. Adv. Mater. **23**(3272–3277), 2011 (2011). doi:10.1002/adma.00507
9. Yang, Y., Gao, P., Gaba, S., Chang, T., Pan, X., Lu, W.: Observation of conducting filament growth in nanoscale resistive memories. Nat. Commun. **3**, 732 (2012). doi:10.1038/ncomms1737
10. Liu, Q., et al.: Real-time observation on dynamic growth/dissolution of conductive filaments in oxide-electrolyte-based ReRAM. Adv. Mater. **24**, 1844–1849 (2012). doi:10.1002/adma.201104104
11. Kudo, M., Arita, M., Ohno, Y., Takahashi, Y.: Filament formation and erasure in molybdenum oxide during resistive switching cycles. Appl. Phys. Lett. **105**, 173504 (2014). doi:10.1063/1.4898773
12. Kudo, M., Arita, M., Takahashi, Y., Ohba, K., Shimuta, M., Fujiwara, I.: Visualization of conductive filament during write and erase cycles on nanometer-scale ReRAM achieved by in-situ TEM. In: Proceedings of 7th International Memory Workshop (IMW), pp. 85–88. IEEE, Piscataway (2015). doi:10.1109/IMW.2015.7150312
13. Fujii, T., Arita, M., Takahashi, Y., Fujiwara, I.: In situ transmission electron microscopy analysis of conductive filament during solid electrolyte resistance switching. Appl. Phys. Lett. **98**, 212104 (2011). doi:10.1063/1.3593494
14. Fujii, T., Arita, M., Takahashi, Y., Fujiwara, I.: Analysis of resistance switching and conductive filaments inside Cu-Ge-S using in situ transmission electron microscopy. J. Mater. Res. **27**, 886–896 (2012). doi:10.1557/jmr.2011.437
15. Kudo, M., Ohno, Y., Hamada, K., Arita, M., Takahashi, Y.: In-situ TEM observation of Cu/MoO_x ReRAM switching. ECS Trans. **58**, 19–25 (2013). doi:10.1149/05805.0019ecst
16. Arita, M., Ohno, Y., Takahashi, Y.: Switching of $Cu/MoO_x/TiN$ CBRAM at MoO_x/TiN interface. Phys. Status Solidi A **213**, 306–310 (2016). doi:10.1002/pssa.201532414
17. Takahashi, A., Ohno, Y., Kudo, M., Nakane, A., Arita, M., Takahashi, Y.: Study on in-situ TEM observation of WO_x ReRAMs with Cu top electrodes. Paper presented at European Material Research Society (EMRS) 2015, Spring Meeting, Congress Center, Lille, 11–15 May 2015
18. Arita, M., Takahashi, A., Ohno, Y., Nakane, A., Tsurumaki-Fukuchi, A., Takahashi, Y.: Switching operation and degradation of resistive random access memory composed of tungsten oxide and copper investigated using in-situ TEM. Sci. Rep. **5**, 17103 (2015). doi:10.1038/srep17103
19. Kudo, M., et al.: Preparation of resistance random access memory samples for in situ transmission electron microscopy experiments. Thin Solid Films **533**, 48–53 (2013). doi:10.1016/j.tsf.2012.10.102
20. Rahama, S.Z., et al.: Excellent resistive memory characteristics and switching mechanism using a Ti nanolayer at the Cu/TaO_x interface. Nano. Res. Lett. **7**, 345 (2012). doi:10.1186/1556-276X-7-345
21. Chen, Y.Y., et al.: Balancing SET/RESET pulse for $>10^{10}$ endurance in HfO_2/Hf 1T1R bipolar RRAM. IEEE Trans. Electr. Dev. **59**, 3243–3249 (2012). doi:10.1109/TED.2012.2218607